Mustansiriyah Journal of Pure and Applied Sciences, Print ISSN: ٢٩٥٧-٩٩١٠. Online ISSN: ٢٩٥٧-٩٩٢٩, Vol. ٢, No. ٤, ٢٠٢٤, Pages ٤٩-٥٨
DOI:

MJPAS

MUSTANSIRIYAH JOURNAL OF PURE AND APPLIED SCIENCES

Journal homepage:
https://mjpas.uomustansiriyah.edu.iq/index.php/mjpas

RESEARCH ARTICLE - PHYSICS

Investigating the Structural and Optical Properties of Pure and Zinc (Zn)-Doped Copper Oxide at Different Weight Ratios

Wessam Mahmood Taher[١*], Ziad .M. Abood[٢] ,Abdulhussan Abas Khadayier[٣].

[١*, ٢] **Department of Physics, College of Education**, Mustansiriyah **University, Iraq**

[٣]**Department of Physics, College of Education, Al-Qadisiyah University, Iraq**

* Corresponding author Email: wessammahmood٧٧@gmail.com, dr.ziadmabood@uomustansiriyah.edu.iq

Article Info.

Article history:

Received
٠٧ March ٢٠٢٤

Accepted
٢١ April ٢٠٢٤

Publishing
٣٠ September ٢٠٢٤

Abstract

This study explores the effect of zinc (Zn) doping on the structural and optical properties of the copper oxide. Nano crystalline copper oxide (CuO) thin films were deposited onto the glass substrates by using a plasma deposition technique. This CuO was then doped with Zn ions at certain weight percentages. The structural and morphological characteristics of both pure and Zn-doped CuO thin films were examined by using X-ray diffraction analysis, field emission scanning electron microscopy (FESEM), atomic force microscopy (AFM) and UV optical spectrometry. From XRD, it was revealed that all thin membranes exhibit multi-crystallization and the crystalline volume of thin films was calculated using Scherrer's formula. The crystal size of the Zn doped CuO changed when compared to the pure CuO due to the Zn size, density strain of CuO lattices and dislocation density. From the results of the FESEM and AFM, presence of the small, spherical-shaped granules in the thin films of pure CuO revealed. However, post-doping results revealed the presence of greater homogeneity in the CuO resulting in a regular granular nature. Furthermore, results of the optical study corroborated the successful doping of the CuO as pure CuO possess highest optical absorption values and the lowest values of the optical band gap. However, post doping results of the CuO showed an increase in optical band gap when the doping rates was less than ٦٪ but shows decrement at relatively higher doping rates revealing the effect of Zn doping on CuO.

The official journal published by the College of Education at Mustansiriya University

Keywords: Radio frequency (RF); sputtering; thin film; CuO; Zn-doped CuO; structural and optical properties
.

١. Introduction

Nowadays, research on metal-doped transition metal oxides and nanostructured metal oxides is drawing researcher's attention [١]. Among different metal oxides, CuO and $Cu_{٢}O$ are commonly used oxides for the preparation of nanoparticles of various sizes and shapes. The properties of these nanostructures depend on the preparation methods and the crystal structure thus obtained [٢]. Consistent with literature, variety of synthesis methods have been reported for the preparation of CuO nanostructures including thermal evaporation [٣], sonochemical synthesis [٤], sol-gel method [٥], chemical vapor deposition, laser ablation, and microwave-assisted synthesis [٦][٧]. Copper oxides are considered an important semiconductor and are being studied as a p-type semiconductor metal with a bandgap of about ١٫٧ eV [٨]. These oxides find extensive uses in variety of applications including solar cells [٩], gas sensing [١٠] and biosensors [١١] due to their easy accessibility, low processing cost, non-toxic nature, and good thermal stability.

The conduction properties of the nonconductive materials directly depend on the band gap that can be controlled by doping/ adding impurity ions such as Zn, Cr, or Ni, etc. to the host material. This doping effect helps to modify the electrical, optical and magnetic properties of the base material. Among the aforementioned dopants, the most widely used dopant is zinc (Zn). It is considered as one of the most effective dopants for copper oxide because the ionic radius of zinc (٠٫٦Å) and copper (٠٫٥٧Å) are close to each other that results in efficient incorporation of zinc ions into the CuO lattice without affecting its crystal structure [١٢]. Many researchers have studied the effect of doping on the structural and optical properties of CuO as Jayaprakash et al. [١٣] reported a decrease in the band gap after doping with zinc ions. Similarly, in another study by Rejith et al. [١٤], the effect of Zn doping on the properties of the CuO nanoparticles was studied. Keeping in view the above discussion, this study aimed (i) to synthesize thin films of pure and doped copper oxide (CuO) by radio-frequency plasma deposition technology and (ii) to investigate the effect of zinc (Zn) doping on the structural and optical properties of the pure copper oxide.

٢. EXPERIMENTAL DETAILS

Herein, a thin film of pure CuO and zinc-doped CuO was deposited on a clean glass substrate using the magnetron sputtering process at a temperature of ٣٥٠ °C. Tablets of Pure copper oxide and also zinc-doped copper oxide was used in different proportions as spray targets with a diameter of ٥cm and a thickness of ٣mm with a flow of argon and oxygen gases (as reactive gasses) at a mixing ratio of ١:٧ inside the deposition chamber. The distance of the target from the substrate was maintained at approximately ١٠ cm. Afterwards, the glass substrates were cleaned with soap and water, followed by drying, and dipping in chromic acid for ٢٤ hours. This was followed by washing it again first with deionized water and then with acetone, and heated in ultrasound waves. Afterwards, the chamber was first emptied of air followed by pumping in the argon and oxygen gases at the pressure of ٢,٥x$١٠^{-٢}$ torr before deposition. The target power was maintained at about ١٠٠ watts, and the deposition time was set to ٢ hours. After sample deposition, the crystal structure of the resulting materials (pure and doped) was then studied through XRD analysis. Field emission scanning electron microscopy (FESEM) and atomic force microscopy (AFM) were also used for morphological/ topographical analysis of the synthesized materials. Furthermore, UV-visible spectrophotometer was used for the optical analysis of the materials.

٣. RESULTS & DISCUSSIONS

٣,١. Crystallographic analysis

Crystallographic results of the pure and doped (١٢٪ zinc doping) CuO thin films are represented in Figure ١a-b and Table ١-٢ respectively. The results of the study revealed that the films examined are a mixture of tenorite crystallised CuO phases and poly-crystalline cubic Cu٢O phases. The two peaks located at ٢Ө of ٤٢,٥° and ٦٢,٢° belong to the (٢٠٠) and (٢٢٠) planes of Cu٢O, respectively (JCPDS٧٧-٠١٩٩). For CuO, there are two main peaks that appear at ٢Ө of ٣٥,٤° and ٣٧,٨° with reflections of (٠٠٢), (١١١) and ٥ small peaks at ٤٧,٣٥°, ٥٢,٧°, ٥٦,٣°, ٦٨,٣٥° and ٧٣,٧° with reflections of (-٢٠٢), (٣١٢), (٠٢١) (-١١٣), ٠٠٤), respectively. According to JCPDS, the intensity of the peaks for CuO increased with Zn doping. It was observed that the improved CuO growth along the trend (١١١), (٠٠٢) It occurs at the expense of $Cu_٢O$. In addition, raising the temperature of the substrate to a level ٣٥٠ °C leads to the instability of the $Cu_٢O$ phase and the films of different phases were obtained [١٥].

Table ١. Crystallite size, dislocation density and strain value of pure CuO films obtained by XRD

Material type	٢ Theta peaks (2θ)	FWHM	D (nm)	d-spacing [Å]	dislocation density δ*$١٠^{-٣}$ ($nm^{-٢}$)	strain across (ε) * $١٠^{-٣}$	Grain size rate (nm)
CuO undoped	٣٣,٠٠٨٣	٠,٢٤	٣٣,١٤٨٠	٢,٧١١٥	٠,٩١٠١	٣,٥٣٤٣	٢٦,٨٥٥٨
	٣٥,٣٧٣٩	٠,٣٦	٢١,٩٥٨٨	٢,٥٢٧٢	٢,٠٧٣٩	٤,٩٢٥٨	
	٣٨,٤٩٥٦	٠,٩٦	٨,١٦٠٠	٢,٣٣٦٦	١٥,٠١٨٤	١١,٩٩٦٣	
	٤٢,٠٥٥٣	٠,١٨	٤٣,٠٢٦٨	٢,١٤٦٧	٠,٥٤٠٢	٢,٠٤٣١	
	٥٦,٣٩٤٥	٠,٤٨	١٥,٢٣٤٨	١,٦٣٠٢	٤,٣٠٨٥	٣,٩٠٦٥	

	٦٧,٠٤٥٦	٠,١٨	٣٨,٤٢٩١	١,٣٩٤٧	٠,٦٧٧١	١,١٨٥٦

Table ٢. Crystallite size, dislocation density and strain value of Zn-doped CuO films obtained by XRD.

Material type	**٢ Theta peaks (2θ)**	**FWHM**	**D (nm)**	**d-spacing [Å]**	**dislocation density δ * ١٠-٣ (nm-٢)**	**strain across (ε) * ١٠-٣**	**Grain size rate (nm)**
(CuO:Zn)١٢٪	٣٥,٤٨١٣	٠,٦	١٣,١٧١٣	٢,٥٢٧٩	٥,٧٦٤٢	٨,١٨٣٢	٢١,٢٦١٤
	٣٧,٢٠٨٧	٠,٣٦	٢١,٨٤٣٨	٢,٤١٤٥	٠,٩٣٧١	٣,٠٢١٤	
	٣٨,٢٣١٤	٠,٢٤	٣٢,٦٦٦٠	٢,٣١٣٨	١,٤٧٠٢	٣,٧٠٧٧	
	٤٣,٣٤٨٣	٠,٧٢	١٠,٧٠٩٤	٢,٠٨٤٦	٨,٧١٩١	٧,٩٠٤٩	
	٥٧,٠٦٦٩	٠,٣	٢٤,٢٩٨٥	١,٦١٢٦	١,٦٩٣٧	٢,٤٠٧٥	
	٦٧,٧١١٥	١,٢	٥,٧٤٢١	١,٣٨٢٦	٣٠,٣٢٩٣	٧,٨٠٥٠	

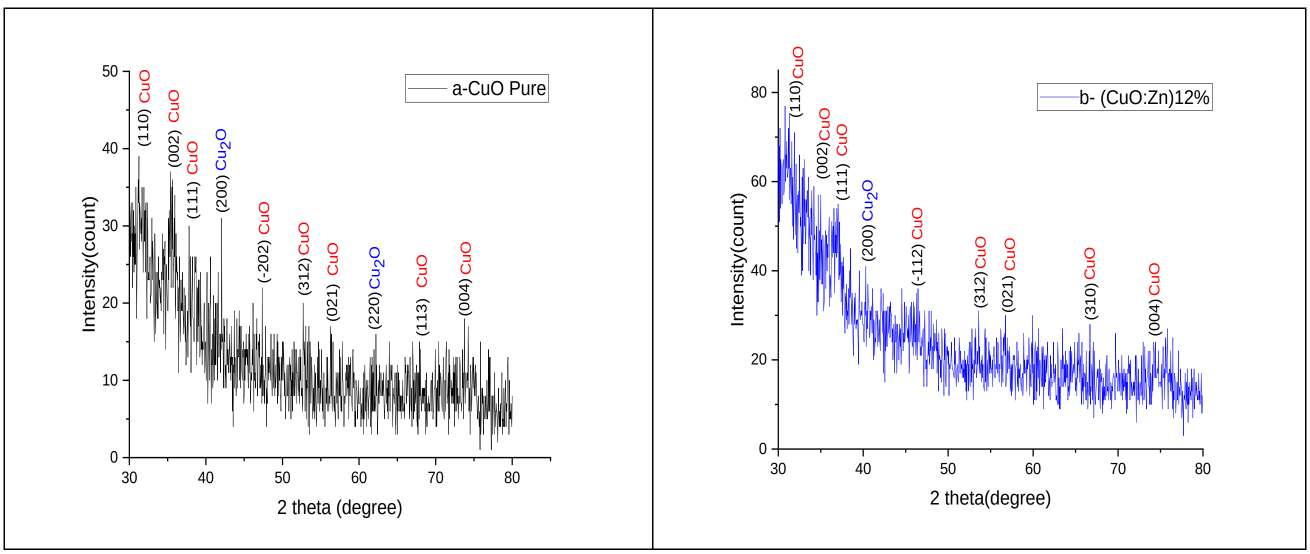

Figure ١(a-b). XRD results of (a) pure and (b) Zn doped CuO films.

From the results obtained in Table ١ for CuO films deposited on glass substrates at a temperature of ٣٥٠Co, the XRD reflections indicate that the lattice parameters were determined using eight reflection lines, where the size of the crystals was calculated using the Debye-Scherer equation [١٦] for copper oxide films deposited with radio frequencies.

$$D = \frac{K\lambda}{\beta cos\theta} \quad (1)$$

Where k is ٠،٩ for the spherical shape that is considered the least distant,(λ) is the wavelength of the X-rays and (β) is the full width of the half-maximum of the peak and. (θ) is the Bragg angle, and the dislocation density was calculated to determine defects in the lattice and micro sole using Eq

$$\delta = \frac{١}{D^{٢}} \quad (٢)$$

$$\boldsymbol{\varepsilon = \frac{\beta}{4tan\theta}} \quad (3)$$

Where, δ refers to the micro-strain and ε is dislocation density.

Results of the XRD analysis revealed that the positions of the XRD peaks shifted slightly towards the right side after doping with zinc. Substituting Zn does not generally change the lattice constants of CuO, but may lead to stress, shrinkage, anisotropy and thus distortion of the lattice. Therefore, compressing stress shifts the diffraction levels to higher angle values [١٧]. This slight change in the diffraction angles is due to the microscopic structure as well as the crystalline size of the nano-copper saturated with Zn, which depends on the doping ratio, as increasing the doping of the zinc led to an increase in the intensity of the peaks at the (١١١) (٠٠٢) levels as corroborated in Figure ١a-b. However, no linear dependence with increasing zinc concentration in the lattice was observed [١٩], because the ionic radius of zinc is nearly ٠,٦ Å, which is close to the ionic radius of copper i.e., ٠,٥٧ Å. Furthermore, it was observed that the size of the crystals decreased with increasing concentration of zinc doping, while the strain increased with the increased zinc ions pressure in the lattice. This led to an obstruction in the growth of the CuO crystal leading to a decrease in the size of the crystals. While on the other hand, at lower zinc concentration, the size of the crystals increases with the decrease in strain leading to the deformation of the network due to stress as a result of the anisotropic contraction of the network.

٣,٢ FE-SEM and AFM

Through microscopic FESEM results of CuO (Figure ٢), it was observed that the copper oxide contains a mixture of atoms having spherical shape with an unequal grain size of between ٧-٥٠ nm. This is due to the variable growth properties of the CuO crystal with a monoclinic structure consisting of oxygen and copper [١٨].

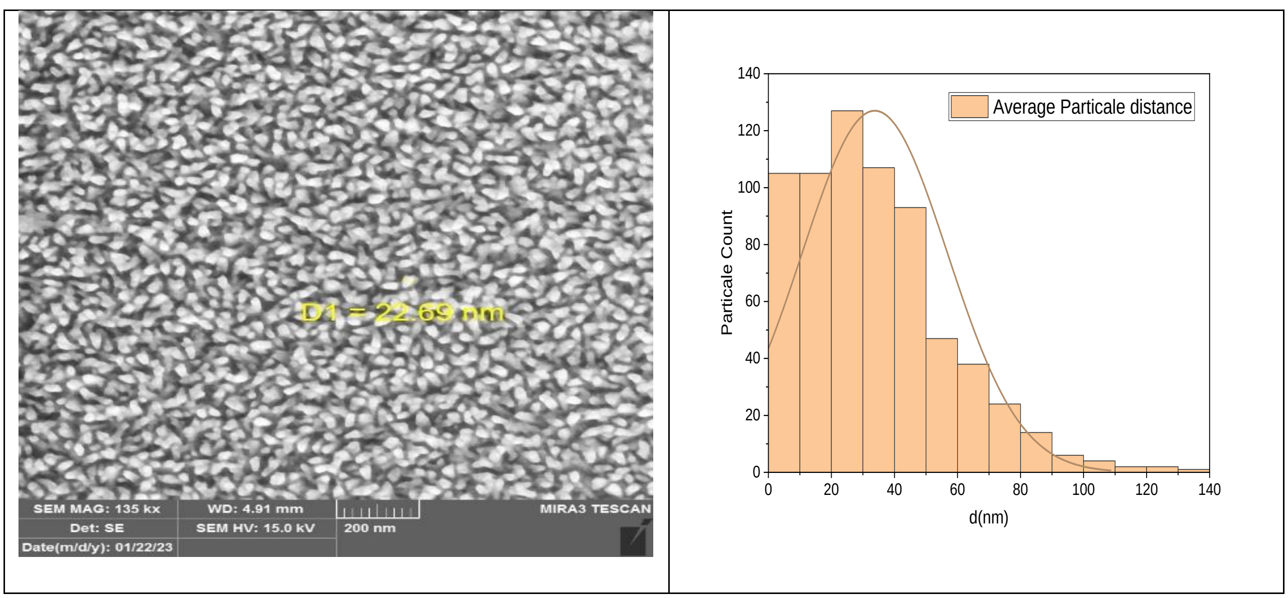

Figure ٢. FE-SEM images of pure CuO films.

Zn doping to CuO (Figure ٣), however, has little effect on CuO morphology. However, the inspection of the FESEM data demonstrates how the Zn doping causes a variation in the size of the CuO particles, leading to the production of tiny nanostructures. Doping with Zn will determine the dimensions and shape of the CuO nanostructure. In Figures ٢-٣, the uniform growth of uniform dispersed single copper oxide crystal was observed with a reduction in the grain size due to tensile stress. Results of the study correlate with already reported literature [١٧].

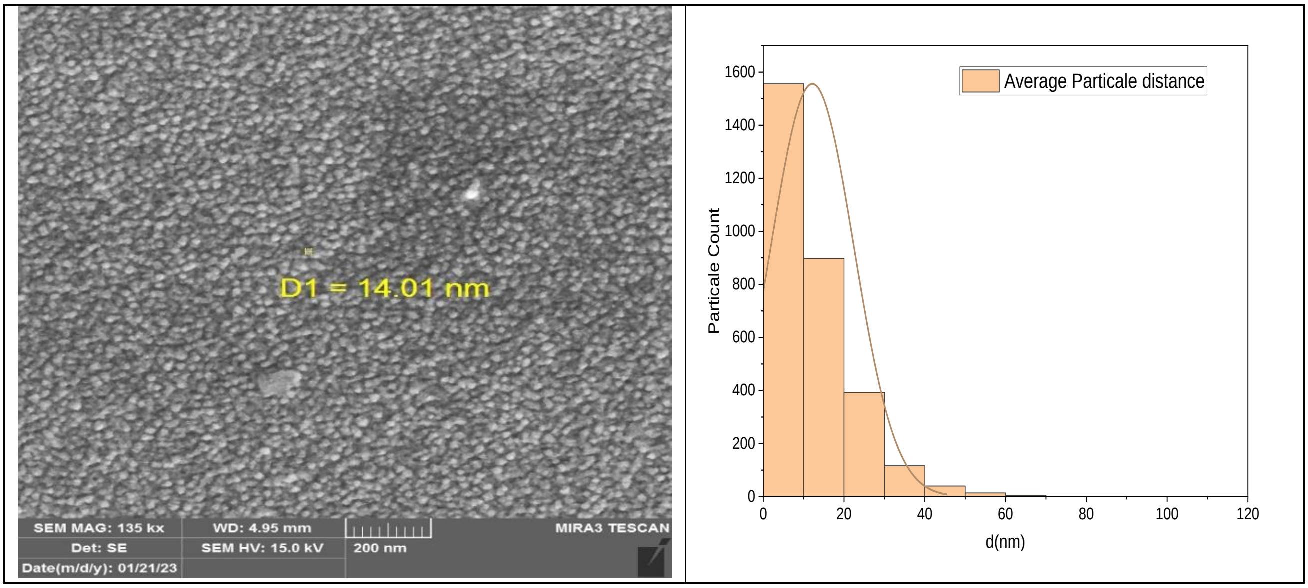

Figure ٣. FESEM images of the Zn doped CuO films.

Microscopic AFM images of the pure copper oxide (Figure ٤) revealed the formation of semi-spherical, nano-sized particles whose distribution is irregular. The surface area relative to volume and high surface energy are responsible for the aggregation.

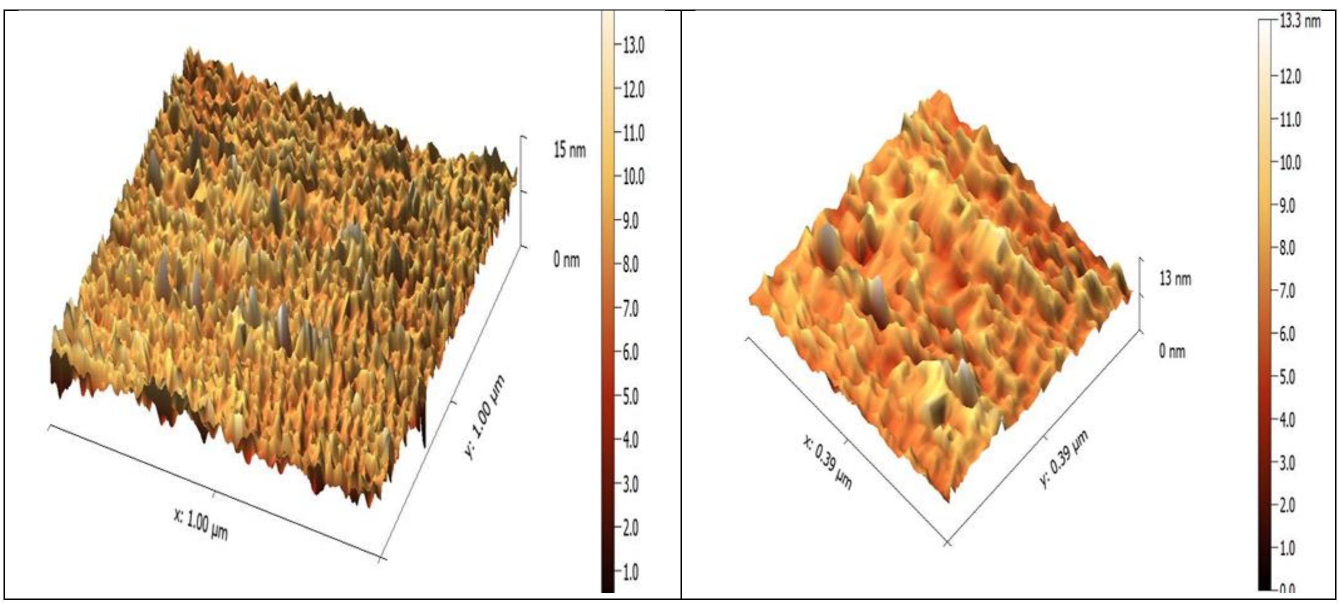

Figure ٤. AFM results of pure CuO films.

However, after Zn doping to copper oxide, the crystalline growth of nanomaterials affected to a greater extent. It is also possible to control the surface morphology of CuO doped with zinc, which is greatly affected by the presence of other ions [١٩][٢٠], where zinc acts to smoothen the CuO surface in the CuO:Zn nanocomposite. However, too much high concentration of zinc ions reduces the surface energy through collection.

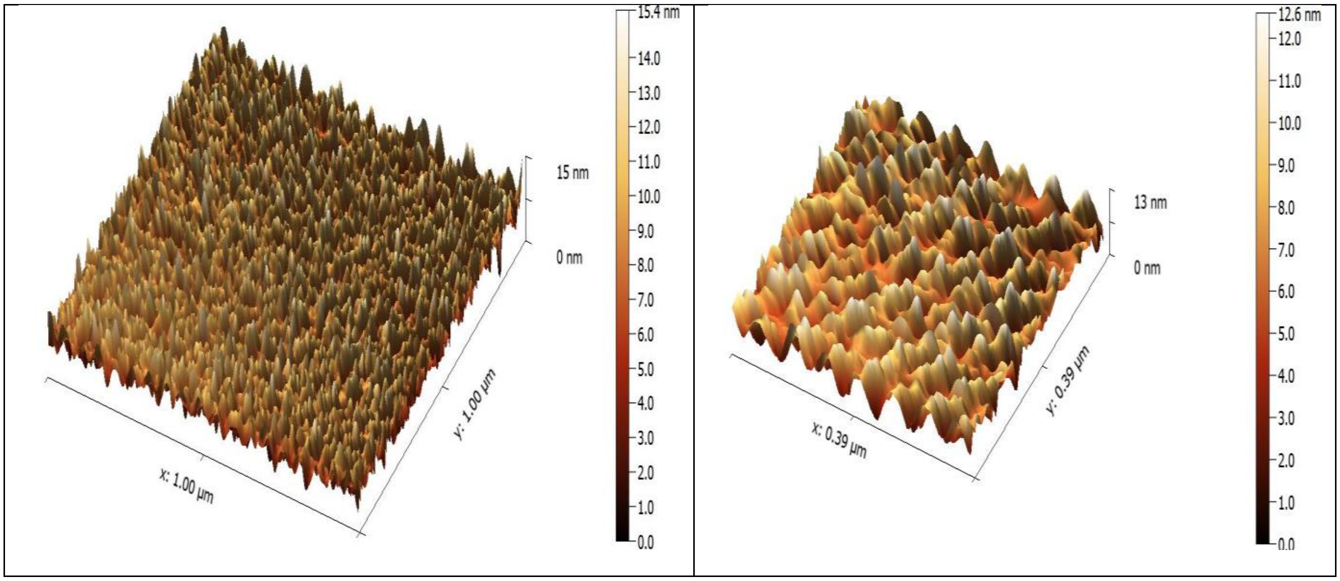

Figure ٥. AFM images of Zn doped CuO films.

The optical properties including absorbance, transmittance, reflectance, and absorption coefficient and band gap; of pure as well as Zn doped CuO thin films were studied to investigate the effect of Zn doping to the properties of the copper oxide films. Results of the study (Figure ٦a) of the absorbance measurements clearly revealed the inverse relation between absorbance and the implantation dose. While on the other hand, Figure ٦b suggests that the pure CuO possess low transmittance when compared with the optical transmittance values of the Zn doped CuO in the visible region. It was found that the highest value comes nearly to ١٠٪ when the Zn doping percentage was ١٢٪ in the visible range. The increase in optical transmittance of the doped material was mainly due to the crystalline nature of the thin films. These changes are consistent with the physical properties of the thin films being studied.

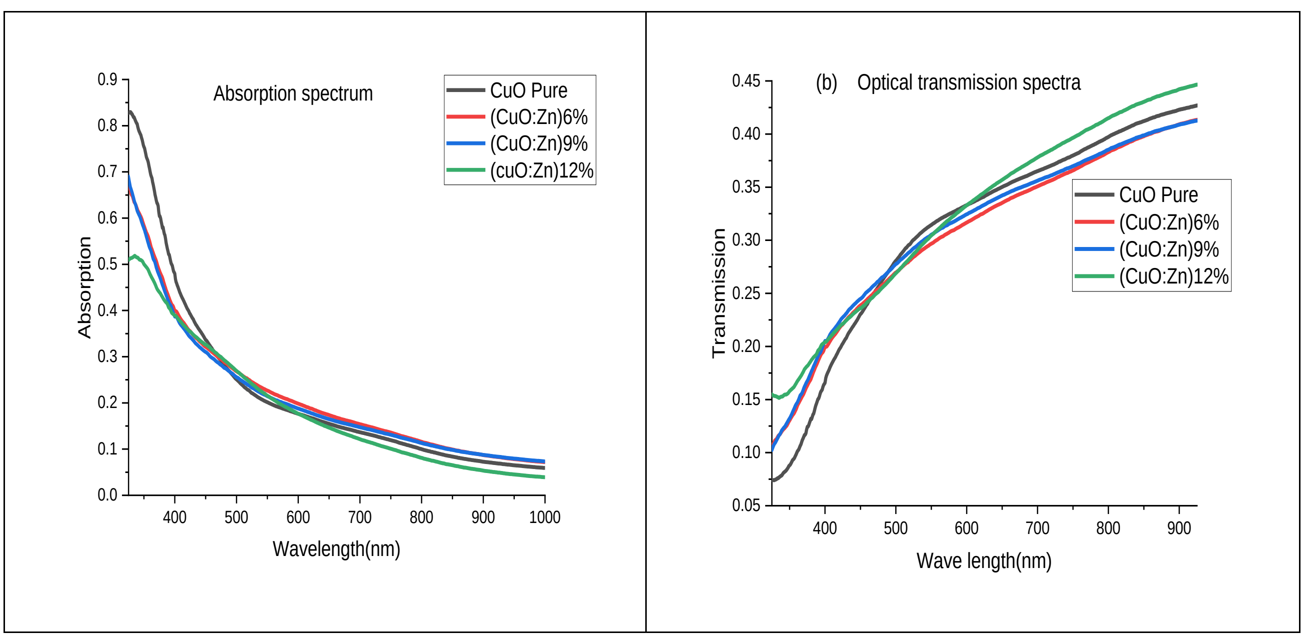

Figure ٦a-b. The relationship between (a) absorbance (b) transmittance against wavelength for pure and doped copper oxide films.

Figure ٧a shows the reflectivity of the synthesized materials (both pure and doped CuO) as a function of wavelength revealing that the reflectivity increases with an increase in short light wavelengths. However, reflectivity increased monotonically with an increase in wavelength. Relation of the absorption coefficient of both pure and doped CuO with wavelength has been summarised in Figure ٧b, the results of the study revealed that the absorption coefficient of (CuO) films doped with zinc decreases with increasing wavelength. The value of the absorption coefficient is high within the limits (١٠^{٤} cm^{-}) suggesting the possibility of direct transfer from the valence band to the conduction band. Further, with an increase in Zn doping, the absorption coefficient creep towards the shorter wavelengths as confirmed from the decline in its value.

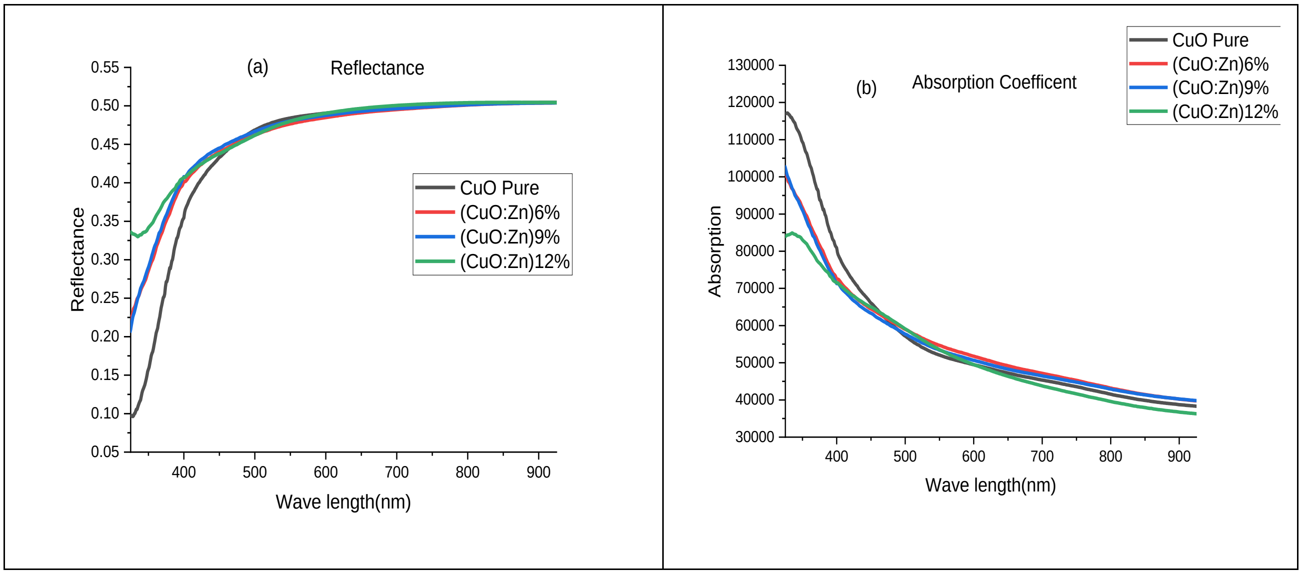

Figure ٧a-b. Relationship between (a) reflectivity (b) absorption coefficient against wavelength for pure and Zn-doped copper oxide films.

The visual properties of both pure and Zn doped CuO nanoparticles are shown in Figure ٨. Optical band gap for CuO particles as ٢,٢٥V. The increase in the energy gap of nanoparticles compared with its bulk counterparts (١,٨٥V) returns to the effect of quantitative size [٢١] because in the case of the bulk matter, energy ranges are effectively form by combining a range of convergent energy levels for atoms. As the particles, approach the nano-volume, the overlapping of adjacent energy levels minimizes that therefore widen the width of energy band. This leads to an increase in the band gap between the parity pack and the plug pack with low particle size. Further, Zn doping to CuO resulted in a decrease of (Eg) to ٢,١٠ eV and the effect can be compounded as a result of the transition from the oxygen ٢p state to d state of Cu and Zn. Overall, the results of the study revealed that the doping of CuO with Zn helps in improving the optical properties of the CuO when compared with the pure CuO and this improvement in optical characteristics is highly dependent on the concentration of Zn ions used for doping [٢٢].

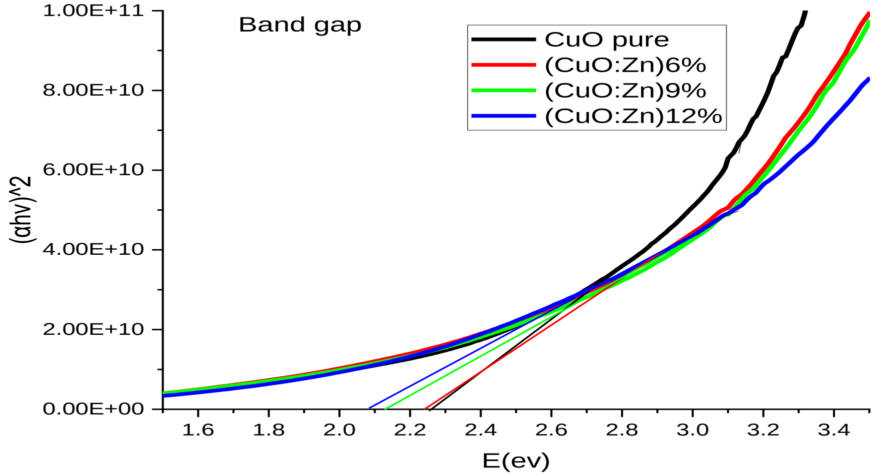

Figure ٨. The relationship between (αhν)^٢ and photon energy for pure and Zn-doped CuO films.

٤. Conclusions

Herein, pure and Zn doped CuO thin films were synthesized by using radio-frequency plasma deposition technology and the variation in the structural and optical behaviour of CuO was investigated both before and after Zn doping. XRD characterization revealed that the prepared films are poly crystalline in mixture of tenorite crystallised CuO and Cu_2O phases. The intensity of the peaks for CuO increased with the doping of zinc. Zn-doped CuO crystal size is highly dependent on the proportion of Zn used for doping as the size of particles reduced due to the replacement of Cu^{2+} ions with Zn^{2+} ions. Further, FESEM analysis also revealed that the size and shape of the doped CuO particles depends mainly on the concentration of zinc in the lattice. Doping of CuO results in making the membrane surface more homogeneous and regular in comparison to the pure CuO films. Additionally, the study of the optical properties of the prepared samples also revealed that increasing the concentration of zinc leads to a decrease in the band gap, and thus improving the electrical conductivity of the material that make them efficient for use in solar cells and optical devices.

٥. Acknowledgments

Mustansiriyah University (www.uomustansiriyah.edu.iq) and Al-Qadisiyah University should be thanked by the authors - Iraq for their assistance with the current project.

٦. References

[١] V. D. Mote, J. S. Dargad, Y. Purushotham, and B. N. Dole, “Effect of doping on structural, physical, morphological and optical properties of Zn١− xMnxO nano-particles,” *Ceram. Int.*, vol. ٤١, no. ١٠, pp. ١٥١٥٣–١٥١٦١, ٢٠١٥.

[٢] X. Fuku, K. Kaviyarasu, N. Matinise, and M. Maaza, “Punicalagin green functionalized Cu/Cu ٢ O/ZnO/CuO nanocomposite for potential electrochemical transducer and catalyst,” *Nanoscale Res. Lett.*, vol. ١١, pp. ١–١٢, ٢٠١٦.

[٣] L. Li, D. Mao, J. Yu, and X. Guo, “Highly selective hydrogenation of CO٢ to methanol over CuO–ZnO–ZrO٢ catalysts prepared by a surfactant-assisted co-precipitation method,” *J. Power Sources*, vol. ٢٧٩, pp. ٣٩٤–٤٠٤, ٢٠١٥.

[٤] S. Sonia, N. D. Jayram, P. S. Kumar, D. Mangalaraj, N. Ponpandian, and C. Viswanathan, “Effect of NaOH concentration on structural, surface and antibacterial activity of CuO nanorods synthesized by direct sonochemical method,” *Superlattices Microstruct.*, vol. ٦٦, pp. ١–٩, ٢٠١٤.

[٥] I. S. Yahia, A. A. M. Farag, S. El-Faify, F. Yakuphanoglu, and A. A. Al-Ghamdi, “Synthesis, optical constants, optical dispersion parameters of CuO nanorods,” *Optik (Stuttg).*, vol. ١٢٧, no. ٣, pp. ١٤٢٩–١٤٣٣, ٢٠١٦.

[٦] M. Fterich, F. Ben Nasr, R. Lefi, M. Toumi, and S. Guermazi, “Effect of concentration of hexamethylenetetramine in structure, microstructure and optical properties of CuO nanoparticles synthesized by hydrothermal route,” *Mater. Sci. Semicond. Process.*, vol. ٤٣, pp. ١١٤–١٢٢, ٢٠١٦.

[٧] J. Singh, S. Sharma, S. Soni, S. Sharma, and R. C. Singh, “Influence of different milling media on structural, morphological and optical properties of the ZnO nanoparticles synthesized by ball milling process,” *Mater. Sci. Semicond. Process.*, vol. ٩٨, pp. ٢٩–٣٨, ٢٠١٩.

[٨] T. Jiang, Y. Wang, D. Meng, X. Wu, J. Wang, and J. Chen, “Controllable fabrication of CuO nanostructure by hydrothermal method and its properties,” *Appl. Surf. Sci.*, vol. ٣١١, pp. ٦٠٢–٦٠٨, ٢٠١٤.

[٩] H. Siddiqui, M. S. Qureshi, and F. Z. Haque, “Valuation of copper oxide (CuO) nanoflakes for its suitability as an absorbing material in solar cells fabrication,” *Optik (Stuttg).*, vol. ١٢٧, no. ٨, pp. ٣٧١٣–٣٧١٧, ٢٠١٦.

[١٠] J.-S. Lee, A. Katoch, J.-H. Kim, and S. S. Kim, “Effect of Au nanoparticle size on the gas-sensing performance of p-CuO nanowires,” *Sensors Actuators B Chem.*, vol. ٢٢٢, pp. ٣٠٧–٣١٤, ٢٠١٦.

[١١] R. Etefagh, E. Azhir, and N. Shahtahmasebi, “Synthesis of CuO nanoparticles and fabrication of nanostructural layer biosensors for detecting Aspergillus niger fungi,” *Sci. Iran.*, vol. ٢٠, no. ٣, pp. ١٠٥٥–١٠٥٨, ٢٠١٣.

[١٢] M. Ashokkumar and S. Muthukumaran, “Effect of Ni doping on electrical, photoluminescence and magnetic behavior of Cu doped ZnO nanoparticles,” *J. Lumin.*, vol. ١٦٢, pp. ٩٧–١٠٣, ٢٠١٥.

[١٣] J. Jayaprakash, N. Srinivasan, P. Chandrasekaran, and E. K. Girija, “Synthesis and characterization of cluster of grapes like pure and Zinc-doped CuO nanoparticles by sol–gel method,” *Spectrochim. Acta Part A Mol. Biomol. Spectrosc.*, vol. ١٣٦, pp. ١٨٠٣–١٨٠٦, ٢٠١٥.

[١٤] S. G. Rejith and C. Krishnan, “Optical characterizations of Zn-doped CuO nanoparticles,” *Sci. Acta*

Xaver, vol. ٤, p. ٩١, ٢٠١٣.

[١٥] M. Shaban, K. Abdelkarem, and A. M. El Sayed, "Structural, optical and gas sensing properties of Cu٢O/CuO mixed phase: Effect of the number of coated layers and (Cr+ S) co-Doping," *Phase Transitions*, vol. ٩٢, no. ٤, pp. ٣٤٧–٣٥٩, ٢٠١٩.

[١٦] N. J. Calos, J. S. Forrester, and G. B. Schaffer, "A crystallographic contribution to the mechanism of a mechanically induced solid state reaction," *J. Solid State Chem.*, vol. ١٢٢, no. ٢, pp. ٢٧٣–٢٨٠, ١٩٩٦.

[١٧] S. Y. Pung, C. S. Ong, K. M. Isha, and M. H. Othman, "Synthesis and characterization of Cu-doped ZnO nanorods," *Sains Malaysiana*, vol. ٤٣, no. ٢, pp. ٢٧٣–٢٨١, ٢٠١٤.

[١٨] Q. Ahsanulhaq, J. H. Kim, J. S. Lee, and Y. B. Hahn, "Electrical and gas sensing properties of ZnO nanorod arrays directly grown on a four-probe electrode system," *Electrochem. commun.*, vol. ١٢, no. ٣, pp. ٤٧٥–٤٧٨, ٢٠١٠.

[١٩] B. Li and Y. Wang, "Facile synthesis and photocatalytic activity of ZnO–CuO nanocomposite," *Superlattices Microstruct.*, vol. ٤٧, no. ٥, pp. ٦١٥–٦٢٣, ٢٠١٠.

[٢٠] M. Ahmad, E. Ahmed, Z. L. Hong, X. L. Jiao, T. Abbas, and N. R. Khalid, "Enhancement in visible light-responsive photocatalytic activity by embedding Cu-doped ZnO nanoparticles on multi-walled carbon nanotubes," *Appl. Surf. Sci.*, vol. ٢٨٥, pp. ٧٠٢–٧١٢, ٢٠١٣.

[٢١] C. Yang, X. Su, F. Xiao, J. Jian, and J. Wang, "Gas sensing properties of CuO nanorods synthesized by a microwave-assisted hydrothermal method," *Sensors Actuators B Chem.*, vol. ١٥٨, no. ١, pp. ٢٩٩–٣٠٣, ٢٠١١.

[٢٢] J. Iqbal *et al.*, "Facile synthesis of Zn doped CuO hierarchical nanostructures: Structural, optical and antibacterial properties," *Aip Adv.*, vol. ٥, no. ١٢, ٢٠١٥.